XLI CILAMCE
XLI Ibero-Latin American Congress on Computational Methods in Engineering
16-19 November, 2020 FOZ DO IGUAÇU PARANÁ - BRAZIL

Wing Structural Optimization for Electric Distributed Propulsion Aircraft using Genetic Algorithm

Bruno Amaral de Oliveira[1], Hélio de Assis Pegado[2]

[1]*Dept. of Mechanical Engineering, Federal University of Minas Gerais*
Presidente Antônio Carlos, 6627, 31270-901, Minas Gerais, Brazil
brunoaero@ufmg.br
[2]*Dept. of Mechanical Engineering, Federal University of Minas Gerais*
Presidente Antônio Carlos, 6627, 31270-901, Minas Gerais, Brazil
helio@demec.ufmg.br

Abstract. The search for less polluting means of transport has been stimulating the development of batteries with higher energy densities and electric motors that are more efficient. These advances have made possible the emergence of several all-electric aircraft, which make use of multiple rotors. In this sense, there was a need to create a methodology to be followed in the conceptual design phase, focused on aerodynamic and structural issues that change in this type of aircraft. These changes, such as the lack of a Gravity Center shift and the need for a greater number of engines and rotors, alters the spar, the aerodynamic flow, the number of ribs and the stiffness of the wing itself. In this study, the engines are distributed along the wing, aiming greater traction and less variation in the angle of attack along the wingspan. An aerodynamic model was created with these requirements, based on the lift line theory, in order to calculate the flight load. Finally, using these values, employing routines of genetic algorithms, the structure was optimized, adopting the spar geometry and thickness as design variables, with the objective of minimizing weight, following the Tsai-Wu criterion and the impossibility of buckling.

Keywords: Optimization; Electric Distributed Propulsion; Spar

1 Introduction

At the beginning of aviation, most of the aircraft needed several engines and rotors to produce sufficient traction for their flight, given the low power available by the combustion engines existing at the time. With the improvement of jet and turboprop propulsion, a reduction trend was seen in this number, mainly due to the great complexity that these engines require, such as electrical, hydraulic and fuel supply, in addition to presenting greater thermal efficiency when used in larger dimensions. However, the need to develop less polluting means of transport, following the goals seated in the 'FlightPath 2050', mentioned in Graham et al. [1], has stimulated the improvement in batteries with higher energy densities and more efficient electric motors, which, according to Moore and Fredericks [2], have great scalability, that is, they are able to present an energy efficiency relatively constant, regardless of its size. This characteristic allows the use of several engines to be resumed, no longer due to the lack of power, but taking the several advantages that the "electric distributed propulsion" (EDP) can provide to the aircraft design. In this sense, several researches have concentrated efforts to establish and quantify what would be the trade-offs of (EDP). This form of propulsion increases the complexity of the project, especially when the motors are positioned on the lifting surfaces. The propellers, when producing traction, change the flow angle and speed, creating vortexes that modify the lift distribution generated by these surfaces. Because of these effects, the variation in the size, spacing and positioning of electrically-driven propellers, according to Moore and Ning [3], can provide greater redundancy against failures, alter structural loading, reduce drag, improve propulsive efficiency, and increase lift during landing and takeoff. Besides that, by distributing the propulsion, the aircraft can produce less noise, cited in Gohardani et al. [4], and combine with differential thrust, create a "virtual rudder", downsizing the vertical tail to reduce weight and drag, according to Reynolds et al. [5].

Therefore, given so many advantages, this paper proposes to study the process of structural optimization of the wing, carried out by using genetic algorithms, of an aircraft that uses the propulsive system known as (EDP). Changes in aerodynamic loading were analyzed and the structure was modeled numerically and using the

finite element method (FEM). To validate the adopted model, data from the CB-10 Thriatlon aircraft was used, considering the replacement of its single combustion engine by several electrically-driven propellers throughout its wingspan.

2 Matematical Model

2.1 Blade Model

First, in order to quantify the performance and the changes in the flow caused by the blades, the propeller model was created using Blade Element Theory (BET). In this theory, each blade is divided into elementary sections dr along its radius. In each element, a balance of forces is applied between lift, drag, traction (dT) and torque (dM) produced, represented, respectively, by eq. (1) and eq. (2):

$$dT = 0.5B\rho cV_{rel}^2(C_{lb}\cos(\phi) - C_{db}\sin(\phi))dr. \tag{1}$$

$$dM = 0.5B\rho cV_{rel}^2(C_{lb}\sin(\phi) + C_{db}\cos(\phi))rdr. \tag{2}$$

Where B represents the number of blades, ρ the air density, c the chord of the element, V_{rel} the air relative velocity to the element, r the distance from the center of rotation, C_{lb} and C_{db} the lift and drag coefficients of the 2D blade airfoil and ϕ the angle between the traction and lift forces.

At the same time, a balance is applied between the axial and angular momentum, defined by eq. (3) and eq. (4), with the tip and hub loss corrections, eq. (5), addressed by El khchine and Sriti [6], represented respectively by the variables F_{tip} and F_{hub}.

$$dT = 4\pi F\rho V_{inf}^2(a+1)ardr. \tag{3}$$

$$dM = 4\pi F\rho V_{inf}^2(a+1)b\Omega r^3dr. \tag{4}$$

$$F = F_{tip} * F_{hub} \tag{5}$$

In which, V_{inf} is the free stream velocity, Ω the angular velocity, a and b the axial and angular inflow factor, r_{hub} the radius of the hub and F_{tip} and F_{hub} defined by:

$$\mathrm{F}_{tip} = \tfrac{2}{\pi}\arccos\left[exp\left(\tfrac{-B(R-r)}{2r\sin(\phi)}\right)\right]; F_{hub} = \tfrac{2}{\pi}\arccos\left[exp\left(\tfrac{-B(r-r_{hub})}{2r\sin(\phi)}\right)\right].$$

Considering the values of C_{lb} and C_{db} for a fixed angle of attack (α), the geometric torsion angle of the blades (θ), was determined by eq. (6). In addition, was established a relationship between the axial and tangential speeds with the relative speed, eq. (7):

$$\theta = \alpha + \arctan\left(\frac{V_{inf}(1+a)}{\Omega r(1-b)}\right). \tag{6}$$

$$V_{rel} = \sqrt{[V_{inf}(1+a)]^2 + [\Omega r(1-b)]^2}. \tag{7}$$

Using eqs. (1) to (4) and eqs. (6) and (7), was developed an iterative process in MATLAB, which solves this non-linear system for each element along the radius of the blade. Thus, defining the values of geometric torsion, traction, torque and the distribution of a and b values. Therefore, with the latters, it was determined the changes in the flow caused by the propeller, due to the induced velocities, shown by eqs. (8) and (9) and Fig. 1, illustrated in D.J. Auld [7]:

$$V_\theta = b\Omega r. \tag{8}$$

$$V_x = V_{inf}(1+a). \tag{9}$$

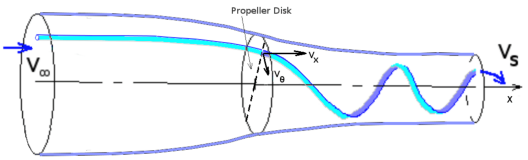

Figure 1. Induced velocity by the blades

2.2 Aerodynamic Model

In order to determine the lift coefficient (C_l) distribution of the wing, an aerodynamic model was developed, in MATLAB, using Prantl's lift line theory, considering a straight wing with the same area as the original aircraft. In this theory, as explained in Houghton et al. [8], the wing is modeled by a superposition of horseshoe vortexes, located in one quarter of the chord, which define the circulation Γ along the span. At each point of analysis, the effective angle of attack of the section (α_{effect}) is determined by eq. (10):

$$\alpha_{effect} = \alpha - \alpha_i. \tag{10}$$

Where α represents the wing geometrical angle of attack and α_i the induced angle of attack.

This is necessary because, unlike 2D sections, the wing, when is generating lift, causes a downwash (ω_i) in the flow, which, coupled with the induced axial and tangential speeds by the propellers in the wing, modify the effective angle of attack in each section, shown in Fig. 2, illustrated in Ferraro et al. [9].

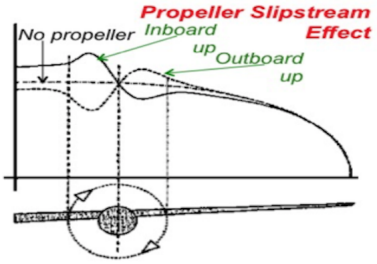

Figure 2. Effects of the Propeller on the wing

For this reason, to take into account the effects of the propellers, an adaptation was used in lift line theory, discussed in Epema [10], in which the induced angle of attack in the wing sections, behind the motors, was determined by eq. (11):

$$\alpha_i = \frac{\omega_i + V_\theta}{V_{inf} + V_x}. \tag{11}$$

With the model defined, a optimization using genetic algorithm, already implemented in MATLAB, was used to determine the distribution of the electrically-driven propellers along the wing, as shown in the Fig. 3.

For this, the quantity, the position, the angular speed and the number of blades of the motors were established as the optimization variables. For each individual, in the population, the performance of the propellers was defined by (BET). With these values, along with the 2D aerodynamic polar of the wing airfoil, the influence coefficients for each point of analysis were calculated, determining the C_l distribution. In each population, the individual with the highest traction, respecting the minimum value required to maintain the flight, obtained in Barros [11], and the smallest variation in the angle of attack along the wingspan, compared to the original C_l distribution, received the best score. Repeating this process, the best individuals of each population reproduce, combining and generating a new different population by the crossover and mutation process, converging to the best combination.

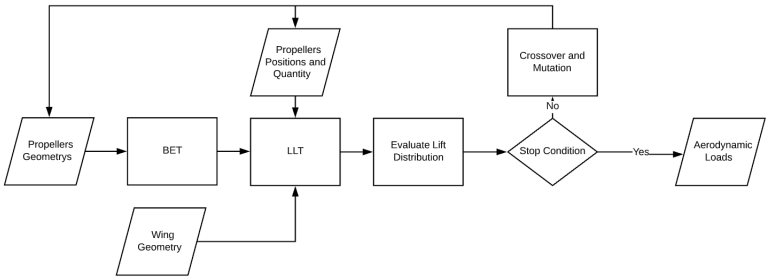

Figure 3. Aerodynamic optimization flowchart

2.3 Flight loads

To calculate the aerodynamic loads, was used the most critical condition in the flight envelope of the CB-10 aircraft, with the load factor $n = +4.87$ and dive speed $(V_d) = 102.2\ m/s$. In this sense, the wing was divided into sections dy along the semi-span (S), as shown by Fig. 4:

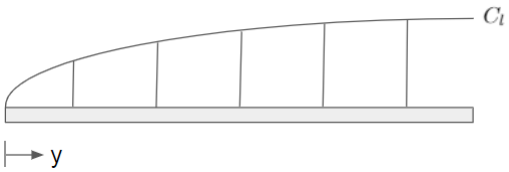

Figure 4. Wing dy

With the C_l distribution, determined by the aerodynamic model, along with the axial velocity V_x, induced by the engines, the elementary lift values dL, for each section, were calculated using the eq. (12), considering $V_x = 0$ for the wing regions outside of the propellers influence.

$$dL(y) = 0.5\rho c_{wing}(V_{inf} + V_x)^2 C_l(y)dy. \tag{12}$$

In which, (c_{wing}) represents the wing chord.

Furthermore, considering the value of the pitching moment coefficient $Cm_{1/4}$ to be constant in $1/4$ of the chord, the shear force (V), the bending moment (M) and the twisting moment (T) were determined by eqs. (13) to (15), respectively:

$$V = \int_0^S dLdy. \tag{13}$$

$$M = \int_0^S Vdy. \tag{14}$$

$$T = \int_0^S 0.5\rho c_{wing}^2(V_{inf} + V_x)^2 Cm_{1/4}dy. \tag{15}$$

Lastly, with the power produced by the electric engines, determined by (BET), its weight was calculated using the $13\ kW/kg$ power density, proposed by Yoon et al. [12]. Combining that weight with the load factor, the inertial forces was determined.

2.4 Wing structure

For the structural model of the aircraft's wing, the spar was designed as a hollow square beam with thin-walls, using composite materials, like the original spar of the CB-10 Thriatlon. As proposed by Zahm [13], the ribs were

distributed following a space of approximately one fifth of the chord, with adaptations to ensure the correct support for the motors.

For dimensioning the structure, a genetic optimization algorithm, already implemented in MATLAB, was used aiming to reduce the structural weight. In this process, represented by the Fig. 5, the thickness of the flange (t_{flange}) and of the web (t_{web}) was varied, as well as the height (h) and width (l), defining the geometric shape of the spar along the span.

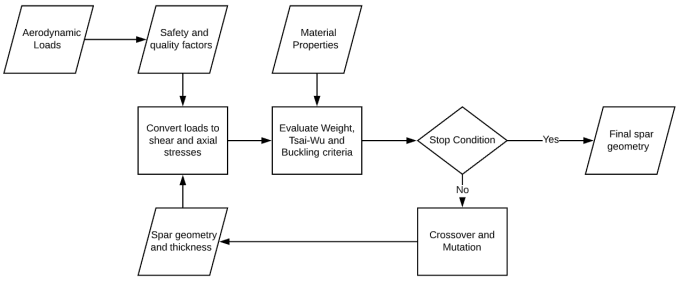

Figure 5. Structural optimization flowchart

In order to ensure that the structures found, during the optimization process, withstand the flight loads, considering the safe margin as 1.5 and quality factor as 1.15, an assessment was made for each individual, evaluating the failure index and the buckling eigenvalue (λ) of the structure, adding a penalization over the spars that failed. In order to identify these failures, each spar was divided, for analysis, into several sections over the span. In each section, along with the aerodynamic loads and the geometrical properties, the values of axial and shear stresses in the plane were calculated. With these stress values, an algorithm was developed, modeled using Tsai-Wu's failure theory, covered in Voyiadjis and Kattan [14], to calculate the failure index. In this sense, the stresses found at each point were compared with the allowable stresses of the material, obtaining the index value, by eq. (16):

$$F_{11}\sigma_{yy}^2 + F_{66}\tau^2 + F_1\sigma_{yy} = Index. \tag{16}$$

Where,

$$\mathrm{F}_{11} = \frac{1}{\sigma_{yy}^T \sigma_{yy}^C}; F_{66} = \frac{1}{(\tau^F)^2}; F_1 = \frac{1}{\sigma_{yy}^T} - \frac{1}{\sigma_{yy}^C}.$$

And, σ_{yy}^T, σ_{yy}^C, τ^F represents the parallel traction, compression and shear failure strength of the material.

In addition, to calculate the local buckling eigenvalue (λ) of the structure, an algorithm was developed, based on the method addressed by Tarjan et al. [15, 16]. In this calculation, a combined request between axial, bending and transverse load was considered, in the web and in the spar flange, created by the aerodynamic forces as well as by the weight and traction produced by the electrically-driven propellers positioned on the wing. For each part, the eigenvalue (λ) was calculated by solving the Rayleigh-Ritz method, represented by eq. (17):

$$\lambda^2 \left[\left(\frac{N_{xb}}{N_{xy,cr}} \right)^2 + \left(\frac{N_{xy}}{Nxy,cr} \right)^2 \right] + \lambda \left(\frac{N_x}{N_{x,cr}} \right) = 1. \tag{17}$$

Where, N_x, N_{xy}, N_{xb} represents the forces per unit length and $N_{(x,cr)}$, $N_{(xy,cr)}$, $N_{(xb,cr)}$ the critical axial, transverse and bending load values for buckling of the structure.

3 Results

The aerodynamic optimization converged in distributing the electric motors, along the wing, with a bigger propeller in the tip, as shown in Fig. 6:

As consequence, the C_l distribution resulted in minor changes, caused by the high value of V_d when compared to the induced velocity by the propellers, as shown in Fig. 7:

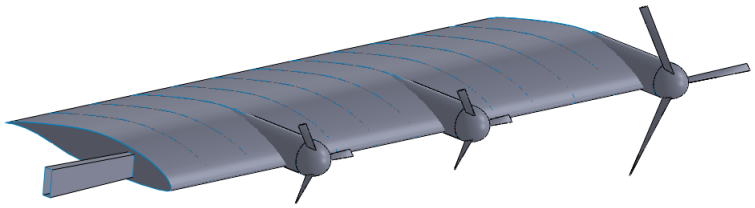

Figure 6. EDP distribution over the semi-span

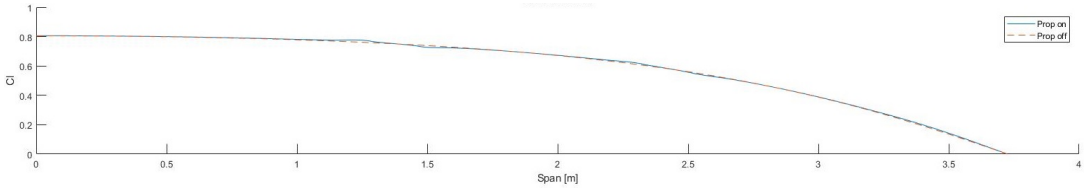

Figure 7. C_l distribution

With that distribution, the spar geometry was defined by the optimization process. To compare with the results from the method developed in MATLAB, the structure was evaluated using HyperWorks Optistruct Finite Element Method (FEM), in the critical flight condition. For that, the wing was modeled using second order 2D quad elements, initially with the size of $12x12$ mm. After performing a convergence test, was used a size of $8x8$ mm. The loads were distributed along the semi-span using RBE3 elements. The result, as shown in the Fig. 8, demonstrate a critical region in the spar upper flange for buckling and Tsai-Wu failure criteria respectively, but confirming that the structure is able to withstand the flight loads. The comparison between the methods results are presented in Table 1:

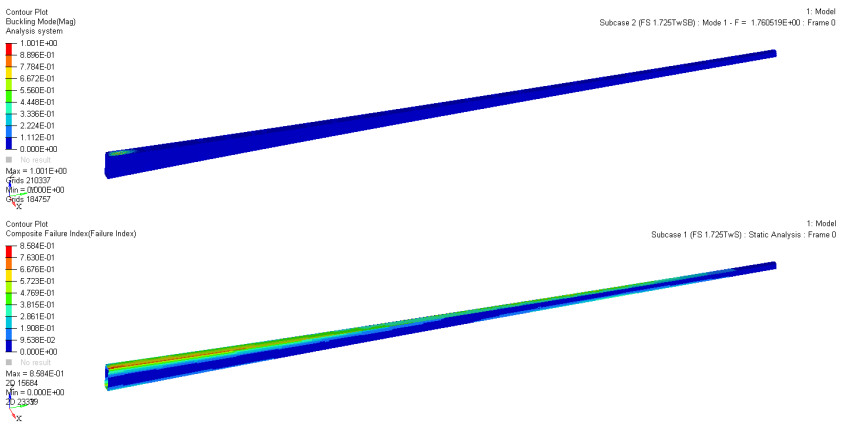

Figure 8. Buckling and Tsai-Wu failure index values in FEM

Table 1. MATLAB and FEM results

Result	Tsai-Wu Index	λ
MATLAB	0.90	1.54
FEM	0.86	1.76

4 Conclusions

As a conclusion, it is possible to observe that there is a good correlation between the data obtained in the model developed in MATLAB, with the analyzes carried out using (FEM), in which the first one presented more conservative results. In addition, compared to the original aircraft, when replacing its single combustion engine with 6 electric motors on the wing, there was a reduction in the shear stress, in the z axis, and in the bending moment, in the x axis. This was due to the effects of the inertial load, during the critical flight condition $n = +4.87$ and speed $V_d = 102.2\ m/s$, that generated forces in the opposite direction to the lift, contributing for a lighter structure.

Acknowledgements. We would like to thank the anonymous referees for their helpful suggestions.

Authorship statement. The authors hereby confirm that they are the sole liable persons responsible for the authorship of this work, and that all material that has been herein included as part of the present paper is either the property (and authorship) of the authors, or has the permission of the owners to be included here.

References

[1] Graham, W., Hall, C., & Morales, M., 2014. The potential of future aircraft technology for noise and pollutant emissions reduction. *Transport Policy*, vol. 34.
[2] Moore, M. & Fredericks, B., 2014. Misconceptions of electric propulsion aircraft and their emergent aviation markets. *52nd AIAA Aerospace Sciences Meeting - AIAA Science and Technology Forum and Exposition, SciTech 2014*.
[3] Moore, K. & Ning, A., 2018. Distributed electric propulsion effects on existing aircraft through multidisciplinary optimization.
[4] Gohardani, A., Doulgeris, G., & Singh, R., 2011. Challenges of future aircraft propulsion: A review of distributed propulsion technology and its potential application for the all electric commercial aircraft. *Progress in Aerospace Sciences*, vol. 47, pp. 369–391.
[5] Reynolds, K., Nguyen, N., Ting, E., & Urnes, J., 2014. Wing shaping concepts using distributed propulsion. *Aircraft Engineering and Aerospace Technology*, vol. 86, pp. 478 – 482.
[6] El khchine, Y. & Sriti, M., 2017. Tip loss factor effects on aerodynamic performances of horizontal axis wind turbine. *Energy Procedia*, vol. 118.
[7] D.J. Auld, K. S., 2020. Aerodynamics for students. `http://www.aerodynamics4students.com/propulsion/blade-element-propeller-theory.php`.
[8] Houghton, E., Carpenter, P., Collicot, S., & Valentine, D., 2013. *Aerodynamics for Engineering Students*. Butterworth-Heinemann.
[9] Ferraro, G., Kipouros, T., Savill, M., Rampurawala, A., & Agostinelli, C., 2014. Propeller-wing interaction prediction for early design.
[10] Epema, H., 2017. Wing optimisation for tractor propeller configurations validation and application of low-order numerical models adapted to include propeller–induced velocities. Master's thesis, Delft University of Technology - Faculty of Aerospace Engineering, Delft, Netherlands.
[11] Barros, C. P., 2001. *Introdução ao projeto de Aeronaves Leves*. UFMG-CEA.
[12] Yoon, A., Yi, X., Martin, J., Chen, Y., & Haran, K., 2016. A high-speed, high-frequency, air-core pm machine for aircraft application. pp. 1–4.
[13] Zahm, A. F., 1920. Relation of rib spacing to stress in wing planes. NACA Technical Note 5, NASA, United States.
[14] Voyiadjis, G. & Kattan, P., 2005. *Mechanics of Composite Materials with MATLAB*. Springer-Verlag.
[15] Tarjan, G., Sapkas, A., & Kollár, L., 2009a. Local web buckling of composite (frp) beams. *Journal of Reinforced Plastics and Composites - J REINF PLAST COMPOSITE*, vol. 29, pp. 1451–1462.
[16] Tarjan, G., Sapkas, A., & Kollár, L., 2009b. Stability analysis of long composite plates with restrained edges subjected to shear and linearly varying loads. *Journal of Reinforced Plastics and Composites - J REINF PLAST COMPOSITE*, vol. 29, pp. 1386–1398.